Chapter 2

Covariant Confined Quark Model

One of the potential objective modern particle physics wants to address is to uncover the underlying structure of hadronic matter. Hence it is of utmost importance to understand the interaction between the constituents of the hadron and their interaction with hadron itself. Understanding heavy-flavor decays is about drawing a distinction between the long-distance (non-perturbative) hadronic effects and short-range (perturbative) QCD dynamics. Short distance dynamics can be easily understood via Wilson's coefficients [13] and effectively evaluated by perturbative approach, whereas the investigations of hadronic matrix elements require nonperturbative approach. It is now believed that hadrons are made up of quarks and gluons degrees of freedom of QCD [118]. To understand the processes such as *Hadronization* (construction of hadron from quarks) and *confinement* (quarks can't exist in isolation), one is required to apply approaches which are essentially non-perturbative because creation and annihilation effects are non-perturbative in nature.

Many attempts have been reported that construct models focusing on different features of QCD. The most model independent approach among these is Light Cone Sum Rule(LCSR) [9,119], where initially the form factors are calculated in large recoil and then extrapolated to zero recoil through pole-type parametrization. Authors of [120] have studied semileptonic decay of $B \to K^* l^+ l^-$ using HQET in low recoil region. Some models describe quark propagation by fully dressed Schwinger functions which wipe out the threshold problem and thus confinement is achieved. These models

use the results obtained from QCD's Dyson-Schwinger's equation [121]. Apart from these, constituent quark model [122], a relativistic quark model [123], QCD relativistic potential model [124], a QCD sum rule technique [125] and covariant constituent quark model (also called covariant quark model(CQM)) [126–128] are some very widely used model approaches out there to accomplish the calculation of hadronic form factors.

It is important to note that the covariant constituent quark model is capable of accounting for the complete physical range of momentum transfer. The covariant quark model described in Refs. [126–128] didn't take into account the quark confinement. The meson transition in CQM are given by covariant Feynman diagrams in which the constituent quarks propagate freely. Vertex functions with suitable damping moderate the UV behaviour of the loop diagrams. The so-called compositeness condition [129, 130] plays an important role in consistent design of the model. Since free particle Green's functions explain the propagation of the constituent quarks, on-shell quark production occurs when the mass of the bound state is more than the sum of the masses of constituent quarks. Consequently, the scope of the covariant quark model's application was restricted to situation where $m_H < m_1 + m_2$. Later, when a universal infrared cutoff parameter was incorporated into the space of loop integrations by [115], this restriction was lifted, thereby introducing infrared confinement. As a result, the CQM can now be employed to describe both heavy and light hadron processes. The Covariant Quark Model is a very versatile tool that can be used to calculate any heavy-heavy, heavy-light and light-light hadron transition once the model parameters are tuned. The prediction of the CQM hold for general mass configurations which is unavailable to the model-independent techniques because they need a heavy quark mass expansion. However, if we use static propagators for the heavy quarks, we can recover the predictions of the heavy-quark expansion.

2.1 Introduction

We have adopted Covariant Confined Quark Model (CCQM) [115–117, 131, 132] for the calculations of weak decays of meson. CCQM takes into account the interaction Lagrangian of meson which interacts with constituent quarks and can be thought of as

a potent quantum field theory technique. Here interaction Lagrangian is constructed in terms of quarks and meson variables and then using Feynman rules, the S-matrix elements that describe the mesonic interaction are derived using set of quark diagrams. Double counting of hadronic degree of freedom is taken care of by compositeness condition Eq. (2.9).

2.2 Framework

The interaction Lagrangian illustrating the coupling between meson $M(q_1\bar{q_2})$ and its constituent quarks q_1 and $\bar{q_2}$ is given by

$$\mathcal{L}_{int}(x) = g_M M(x) \cdot J_M(x) + H.c. \tag{2.1}$$

here g_M represents the coupling strength of meson with its constituent quarks. J_M is the interpolating quark current and is given by

$$J_M(x) = \int dx_1 \int dx_2 F_M(x : x_1, x_2)\bar{q_2}(x_2)\Gamma_M q_1(x_1) \tag{2.2}$$

here Γ_M are the Dirac matrices that are chosen precisely to characterise the associated spin and flavor quantum number of mesonic field $M(x)$. $\Gamma_M = I$ for scalar, $\Gamma_M = \gamma^5$ for pseudoscalar and $\Gamma_M = \gamma^\mu$ is for vector meson. $F_M(x, x_1, x_2)$ is the vertex function and represents the finite size of the meson. For any given four-vector a, vertex function must obey $F_M(x+a, x_1+a, x_2+a) = F_M(x, x_1, x_2)$ so that translational invariance will be achieved for the interaction Lagrangian given in Eq. (2.1). F_M is also associated with the scalar part of Bethe-Salpeter amplitude. Vertex function is chosen to be

$$F_M(x, x_1, x_2) = \delta^{(4)}\left(x - \sum_{i=1}^{2} w_i x_i\right) \Phi_M((x_1 - x_2)^2) \tag{2.3}$$

The correlation function of the two constituent quarks with masses m_1 and m_2 is given by Φ_M and w_i is given by $w_i = m_i/(m_1+m_2)$ which implies that $w_1+w_2 = 1$, where m_i represents the quark mass. For bound state of meson, Bethe-Salpeter equation [121] is used to obtain the Fourier Transform of the correlation function and is denoted by

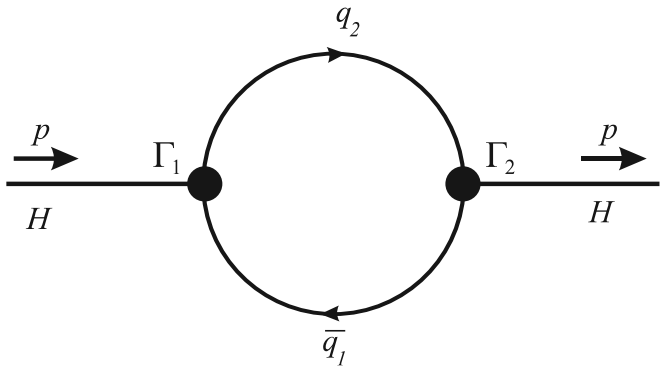

Figure 2.1: One loop self energy diagram

$\Phi_M(-p^2)$. Authors of [133] have shown that one can have any functional form for vertex function, we still choose Gaussian form as will have an extra advantage as it is more analytically easy to handle. The vertex functions is given as

$$\Phi_M(-p^2) = \exp(p^2/\Lambda_M^2) \tag{2.4}$$

The argument of Φ_M contains minus sign which indicates that one is working in Minkowski space. In Euclidean space, p^2 converts to $-p^2$ and so Eq. (2.4) has the fall-off behaviour sufficient enough to overthrow the Ultraviolet divergences of the loop integral. Here Λ_M characterizes the finite size of the meson.

Quark loop diagram in Fig. 2.1 is evaluated using free local fermion propagator for the constituent quarks of the form

$$S_q(k) = \frac{1}{m_i - \not{k}} \tag{2.5}$$

where m_i is the effective constituent quark mass. Now with the help of Fourier transformed vertex function given in Eq. (2.4) and quark propagator defined in Eq. (2.5), we can define meson mass function for diagram shown in Fig. 2.1 as

For pseudoscalar meson

$$\Pi_p(p^2) = N_c g_p^2 \int \frac{d^4k}{(2\pi)^4 i} \Phi_P^2(-k^2) \mathrm{tr}(\gamma^5 S_1(k + w_1 p)\gamma^5 S_2(k - w_2 p)) \tag{2.6}$$

For vector meson

$$\Pi_V^{\mu\nu}(p^2) = N_c g_V^2 \int \frac{d^4k}{(2\pi)^4 i} \Phi_V^2(-k^2) \mathrm{tr}(\gamma^\mu S_1(k + w_1 p)\gamma^\nu S_2(k - w_2 p)) \tag{2.7}$$

Fock representation is used to convert loop momenta to the derivative of external momenta [134,135]. $N_c = 3$ denotes the number of colors and in case of vector meson $\epsilon_V \cdot p = 0$, because it is on its mass-shell, hence the part of the vector mass function which is proportional to $g_{\mu\nu}$ is only required. Hence

$$\Pi_V(p^2) = \frac{1}{3}\left(g_{\mu\nu} - \frac{p_\mu p\nu}{p^2}\right)\Pi_V^{\mu\nu}(p) \tag{2.8}$$

The coupling constant g_M in Eq. (2.1) can be obtained using compositeness condition [129,130], which sets wave function renormalization constant (Z_M) of the meson field to be equal to zero, i.e.

$$Z_M = 1 - \Sigma_M^{'}(m_M^2) = 0 \tag{2.9}$$

$Z_M = 0$ is the so-called compositeness condition, where Z_M is the wave-function renormalization constant, which mathematically connects the bare state and physical state through the following relation

$$|bare\rangle = \sqrt{Z_M}|phys\rangle$$

The bare state interacts with the quantum vacuum to produce the physical state. A "dressed" physical state results from these interactions, involves the emission and reabsorption of virtual particles. Z_M basically quantifies how much of this dressing is present. Z_M can also be looked at as the probability amplitude for the physical state to be found in the bare state. Specifically Z_M gives the residue at the pole in the propagator of the particle which in a way gives the idea about the strength of the coupling constant of the meson with its constituents.

The renormalization constant $\sqrt{Z_M}$ can also be interpreted as the matrix element between the bare and physical state and hence the condition $Z_M = 0$ suggests that physical state doesn't contain the bare state and hence can be considered as an appropriate bound state. $Z_M = 0$ ensures that we avoid the double counting of meson degree of freedom. $\Sigma_M^{'}(m_M^2)$ is the derivative of the mass operator associated with

the self-energy diagram of Fig. 2.1 and is given by

$$\Sigma_M^{'}(m_M^2) = \frac{3g_M^2}{4\pi^2}\Pi_M^{'}(m_M^2) = \frac{3g_M^2}{4\pi^2}\frac{d\Pi_M(p^2)}{dp^2} \tag{2.10}$$

Eq. (2.9) allows us to fully describe the meson interaction via constituent quarks with local constituent quark propagators only, where the derivative of mass operator is taken on mass-shell $p^2 = m_M^2$. Now to calculate the derivative of the mass operators given in Eq. (2.6) − (2.7) we use following identities.

$$\begin{aligned}\frac{d\Pi_M(p^2)}{dp^2} &= \frac{1}{2p^2}p^\mu\frac{d\Pi_M(p^2)}{dp^2},\\ p^\mu\frac{d}{dp^\mu}S(k+wp) &= wS(k+wp)\not{p}S(k+wp)\end{aligned} \tag{2.11}$$

Following the above equations, the derivatives of the mass functions of meson can be expressed as:

For pseudoscalar meson

$$\begin{aligned}\Pi_p^{'}(p^2) = \frac{1}{2p^2}\frac{3g_P^2}{4\pi^2}\int\frac{dk}{4\pi^2 i}\Phi_P^2(-k^2)\Big(&w_1\mathrm{tr}[S_1(k+w_1p)\not{p}S_1(k+w_1p)\gamma^5 S_2(k-w_2p)\gamma^5]\\ &- w_2\mathrm{tr}[S_1(k+w_1p)\gamma^5 S_2(k-w_2p)\not{p}S_2(k-w_2p)\gamma^5]\Big)\end{aligned} \tag{2.12}$$

For vector meson

$$\begin{aligned}\Pi_V^{'}(p^2) = &\frac{1}{2p^2}\frac{1}{3}\Big(g^{\mu\nu} - \frac{p^\mu p^\nu}{p^2}\Big)\\ &\times\int\frac{dk}{4\pi^2 i}\Phi_V^2(-k^2)\Big(w_1\mathrm{tr}[S_1(k+w_1p)\not{p}S_1(k+w_1p)\gamma_\mu S_2(k-w_2p)\gamma_\nu]\\ &- w_2\mathrm{tr}[S_1(k+w_1p)\gamma_\mu S_2(k-w_2p)\not{p}S_2(k-w_2p)\gamma_\nu]\Big)\end{aligned} \tag{2.13}$$

Next step is to solve for the loop integrations shown in Eq. (2.6) − (2.7).

2.2.1 Loop Integration Technique

Let's consider n local propagators $S_i(k+v_i)$ and n Gaussian vertex functions $\Phi_i(-(k+v_{i+n})^2)$ for n point one loop diagram. One loop diagram in Minkowski space can be

stated as

$$I_n(p_1, ..., p_n) = \int \frac{d^4k}{\pi^2 i} \mathrm{tr} \prod_{i=1}^{n} \Phi_i(-(k + v_{i+n})^2) \Gamma_i S_i(k + v_i) \tag{2.14}$$

here linear combinations of external momenta p_i is represented by v_i, whereas k is the loop momenta and Γ_i are the Dirac matrices for i^{th} hadron. The choice of external momenta satisfies $\sum_{i=1}^{n} p_i = 0$. For any four vector a, the integral in Eq. (2.14) will be invariant if loop momenta k is shifted as $k \to k + l$, due to translational invariance of the one loop integral. Any linear combination of external momenta p_i may serve as the four vector a.

Next we apply Fock-Schwinger parameterizations to local quark propagators using

$$\frac{1}{AB} = \int_0^\infty d\beta_1 \int_0^\infty d\beta_2 \exp(-\beta_1 A - \beta_2 B) \tag{2.15}$$

and we get

$$S_i(k + v_i) = (m_i + \not{k} + \not{v}_i) \int_0^\infty d\beta_i \exp[-\beta_i (m_i^2 - (k + v_i)^2)] \tag{2.16}$$

Fock-Schwinger representations are important because they are helpful in performing tensor loop integrals by converting loop momenta into derivatives of the exponent function. Next we use Wick rotation given by

$$k_0 = e^{i\frac{\pi}{2}} k_4 = ik_4 \tag{2.17}$$

on the loop momenta to convert them from Minkowski space to Euclidean space hence $k^2 = k_0^2 - \bar{k^2} = -k_4^2 - \bar{k^2} = -k_E^2 \leq 0$. Now for the quadratic form in Eq. (2.16) to be positive-definite, all external momenta must also be rotated, i.e $v_0 \to iv_4$ and hence $v^2 = -v_E^2$ so that

$$m_i^2 - (k + v_i)^2 = m_i^2 + (k_E + v_{iE})^2 > 0 \tag{2.18}$$

so that the integral over β in Eq. (2.16) is convergent. All the loop integrations are evaluated in Euclidean space. However, we still use Minkowski notation to avoid rewriting the equations. It is to be noted that $k^2 \leq 0$ and $v^2 \leq 0$. By choosing

Gaussian form for the vertex function we have

$$\Phi_i(-(k+v_{i+n})^2) = \exp[\beta_{i+n}(k+v_{i+n})^2] \tag{2.19}$$

where $i = 1, 2, .., n$. Size parameter for meson is denoted by $\beta_{i+n} = s_i = 1/\Lambda_i^2$.

Next using the vertex function representation in Eq. (2.19) and quark propagator in Eq. (2.16), the one loop integration can be written as

$$I_n(p_1, ..., p_n) = \int \frac{d^4k}{\pi^2 i} \mathrm{tr} \prod_{i=1}^{n} \int_0^\infty d\beta_i e^{-\beta_i m_i^2} (m_i + \not{k} + \not{\psi}_i) \exp\{\sum_{i=1}^{2n} \beta_i (k+v_i)^2\}$$

One can see that exponential function in the above equation takes the form of $\beta k^2 + 2kr + z_0$, where $\beta = \sum_{i=1}^{2n} \beta_i$, $r = \sum_{i=1}^{2n} \beta_i v_i$ and $z_0 = \sum_{i=1}^{2n} \beta_i v_i^2$.

Using following properties

$$\begin{aligned} k^\mu \exp(\beta k^2 + 2kr + z_0) &= \frac{1}{2} \frac{\partial}{\partial r_\mu} \exp(\beta k^2 + 2kr + z_0) \\ k^\mu k^\nu \exp(\beta k^2 + 2kr + z_0) &= \frac{1}{2} \frac{\partial}{\partial r_\mu} \frac{1}{2} \frac{\partial}{\partial r_\nu} \exp(\beta k^2 + 2kr + z_0) \end{aligned} \tag{2.20}$$

$\not{k}$ can be replaced by $\not{\partial}_r = \gamma^\mu \frac{\partial}{\partial r_\mu}$ so that one can perform tensor integration for differentiation of the Gaussian exponent. So now loop integral can be re-written as

$$I_n(p_1, ..., p_n) = \int \frac{d^4k}{\pi^2 i} \mathrm{tr} \prod_{i=1}^{n} \int_0^\infty d\beta_i e^{-\beta_i m_i^2} (m_i + \not{\psi}_i + \not{\partial}_r) \exp\{\beta k^2 + 2kr + z_0\} \tag{2.21}$$

Next step is to perform the loop integration and to move the Gaussian exponent $e^{-r^2/\beta}$ to the left through the differential operator using

$$\begin{aligned} \frac{\partial}{\partial r_\mu} e^{-r^2/a} &= e^{-r^2/a} \Big[-\frac{2r^\mu}{a} + \frac{\partial}{\partial r_\mu} \Big] \\ \frac{\partial}{\partial r_\mu} \frac{\partial}{\partial r_\nu} e^{-r^2/a} &= e^{-r^2/a} \Big[-\frac{2r^\mu}{a} + \frac{\partial}{\partial r_\mu} \Big] . \Big[-\frac{2r^\nu}{a} + \frac{\partial}{\partial r_\nu} \Big] \end{aligned} \tag{2.22}$$

and the following commutation relation is used to move the derivatives to the right

$$\Big[\frac{\partial}{\partial r_\mu}, r^\nu \Big] = g^{\mu\nu} \tag{2.23}$$

Using the identity

$$-\frac{r^2}{\beta}+\sum_{i=1}^{2n}\beta_i v_i^2=\frac{1}{\beta}\sum_{1\leq i<j\leq 2n}\beta_i\beta j(v_i-v_j)^2$$

the loop integral shapes like

$$\begin{aligned}I_n(p_1,..,p_n)=\prod_{i=1}^{n}\int_0^\infty\frac{d\beta_i}{\beta^2}\exp\Big\{-\sum_{i=1}^{n}\beta_i m_i^2+\frac{1}{\beta}\sum_{1\leq i<j\leq 2n}\beta_i\beta j(v_i-v_j)^2\Big\}\\ \times\mathrm{tr}\prod_{i=1}^{n}\Gamma_i\Big(m_i+\not{p}_i-\frac{1}{\beta}\not{r}+\frac{1}{2}\not{\partial}_r\Big)\end{aligned}\tag{2.24}$$

The necessary commutation relations have been carried out using FORM code [136] which treats all commutation relations in reliable manner. Now the integral which remains to be evaluated over the Fock-schwinger parameter $0\leq\beta_i<\infty$. By introducing an additional integral they can be converted into a simplex using the transformation [137].

$$\int_0^\infty d^n\beta F(\beta_1,..,\beta_n)=\int_0^\infty dt t^{n-1}\int d^n\alpha\delta\Big(1-\sum_{i=1}^{n}\alpha_i\Big)F(t\alpha_1,...,t\alpha_n)\tag{2.25}$$

The final form of the one loop n point diagram takes the following form

$$\begin{aligned}I_n(P_1,..,P_n)=\int_0^\infty dt\frac{t^{n-1}}{(s+t)^2}\int d^n\alpha\delta\Big(1-\sum_{i=1}^{n}\alpha_i\Big)\exp\Big\{-tz_{loc}+\frac{st}{s+t}z_1+\frac{s^2}{s+t}z_2\Big\}\\ \times\mathrm{tr}\prod_{i=1}^{n}\Gamma_i\Big(m_i+\not{p}_i-\frac{1}{s+t}\not{r}+\frac{1}{2}\not{\partial}_r\Big)\end{aligned}\tag{2.26}$$

here

$$z_{loc}=\sum_{i=1}^{n}\alpha_i m_i^2-\sum_{1\leq i<j\leq n}\alpha_i\alpha_j A_{ij}$$

$$z_1=\sum_{i=1}^{n}\alpha_i\sum_{j=n+1}^{2n}\bar{\beta}_j A_{ij}-\sum_{1\leq i<j\leq n}\alpha_i\alpha_j A_{ij}$$

$$z_2 = \sum_{n+1 \leq i < j \leq 2n} \bar{\beta}_i \bar{\beta}_j A_{ij}$$

$$r = t \sum_{i=1}^{n} \alpha_i v_i + s \sum_{i=n+1}^{2n} \bar{\beta}_i v_i$$

Where $\bar{\beta_{i+n}} = s_i/s,\ s = \sum_{i=1}^{n} s_i.\ \ A_{ij} = (v_i - v_j)^2 (1 \leq i, j \leq 2n)$ and is entirely dependent on the invariant variables.

Entire process of n-point one loop integration involves n numerical integrations, $n-1$ α-parameter integrations and an additional integration for simplex conversion over the scale parameter t. The final integration is done using Mathematica. In Eq. (2.26) if $z_{loc} \leq 0$ the integration over parameter t will not converge due to large t sector.

After applying the above technique to the derivative of meson mass operator given by Eq. (2.12), the final form of the derivative of meson mass function is given by

$$\begin{aligned}
\Pi'_M(p^2) &= \frac{3g_m^2}{4\pi^2} \int_0^\infty \frac{dtt}{a_M^2} \int_0^1 d\beta e^{-tz_0 + z_M} f_M(t, \beta), \\
z_0 &= am_1^2 + (1-\beta) m_2^2 \beta (1-\beta) p^2, \\
z_M &= \frac{2s_M t}{2s_M + t} (\beta - w_2)^2 p^2 \\
a_M &= 2s_M + t, b = (\beta - w_2) t.
\end{aligned} \tag{2.27}$$

The convergence of the integral above the threshold value $p^2 \geq (m_1 + m_2)^2$ (i.e. $z_0 \leq 0$) can be achieved by addition of a small imaginary mass to the quark mass, i.e. $m_i \to m_i - i\epsilon$, $\epsilon > 0$ in the local fermion quark propagator Eq. (2.5). It will rotate the integration variable t to the imaginary axis $t \to it$ and hence the integral Eq. (2.27) turns out to be convergent but carries the imaginary part associated with quark pair production. One of the techniques to get rid of all the conceivable thresholds present in the quark diagram is to introduce an infrared cut-off parameter λ [115].

2.2.2 Infrared Confinement

By introducing the infrared cut-off parameter λ as in Eq. (2.28), one can truncate the scale of the integration to the upper limit and all conceivable thresholds in the primary quark diagram can be eliminated

$$\int_0^\infty dt(...) = \int_0^{1/\lambda^2} dt(...) \tag{2.28}$$

The quark flavor dynamics dominates the low energy meson properties at intermediate scales only say between a confinement scale of few hundred MeV to 1 GeV due to the fact that chiral symmetry is dynamically broken just in this region [**?**]. The cut-off parameter can be considered as a scale upto which quarks have been integrated out hence preventing the determinant in the quark loop diagram to suffer from quark-anti quark thresholds. It is shown in that in applying the IR cut-off of this form [**?**]

$$\lambda_P = [m_c\theta(m - m_c) + m\theta(m_c - m)] \times \theta(P^2 - 4m_c^2)\sqrt{\frac{P^2}{4m_c^2} - 1}$$

if the model parameter m_c is less than the constituent quark mass then the denominator of quark loop diagram is free from divergences. we have chosen this model parameter as an IR-cut off parameter in our study. It is also shown in the same study [**?**] that introduction of the IR cut-off of this particular form does not significantly changes the constituent quark mass. The difference in the quark is less than 50 MeV. Let's illustrate the implementation of confinement using a scalar one-loop propagator. The Schwinger parametrization of the propagator is given by

$$\frac{1}{m^2 - p^2} = \int_0^\infty d\alpha \exp[-\alpha(m^2 - p^2)]$$

Now, let's propose an upper integration limit $1/\lambda^2$ instead of integrating from 0 to ∞. The parameter λ is known as infrared confinement constant with the dimension of mass m. The cut-off allows us to construct a complete function that may be understood as a localised propagator, which reads as

$$\int_0^{1/\lambda^2} d\alpha \exp[-\alpha(m^2 - p^2)] = \frac{1 - \exp[-(m^2 - p^2)/\lambda^2]}{m^2 - p^2} \tag{2.29}$$

Above equation suggests that it is free of singularities in the finite p^2 plane, which signifies that no free quark exists in the asymptotic region of configuration states. The usage of constrained propagator in the shape of whole function, on the other hand, presents its own unique set of challenges. Once the hadron masses and energies of the equation have been fixed, the convolution of whole function causes an accelerated growth of the physical matrix element. This expansion can be thought of as mushrooming and hence the numerical results become extremely sensitive to variations in the parameters those are being chosen which demands for extreme fine-tuning. Hence it is advisable to proceed in the following manner.

Let's start with general m-loop Feynman diagram with n propagators. The Schwinger parametrizations reads

$$\prod(p_1, ..., p_2) = \int_0^\infty d^n\alpha \int [d^4k]^l \Phi \exp[-\sum_{i=1}^{n} \alpha_i(m_i^2 - p_i^2)]$$

here Φ represents the numerator product between propagators and vertex functions. The result of the loop integration provides

$$\prod = \int_0^\infty d^n\alpha F(\alpha_1, .., \alpha_n)$$

Here F represents the structure of a given one loop diagram. All α_i's can be converted into a simplex by using additional t-integration through the identity

$$1 = \int_0^\infty dt\delta(t - \sum_{i=1}^{n} \alpha_i)$$

which leads to

$$\prod = \int_0^\infty dt t^{n-1} \int_0^1 d^n\alpha\delta\Big(1 - \sum_{i=1}^{n} \alpha_i\Big) F(t\alpha_1, ..., t\alpha_n)$$

Now as described in Eq. (2.29), we truncate the upper integration at $1/\lambda^2$ to obtain

$$\prod_{cut-off} = \int_0^{1/\lambda^2} dt t^{n-1} \int_0^1 d^n\alpha\delta\Big(1 - \sum_{i=1}^{n} \alpha_i\Big) F(t\alpha_1, ..., t\alpha_n)$$

Because of the incorporation of the infrared cutoff, the quark loop diagram is now

completely devoid of any and all conceivable thresholds. We will assume the same numerical value of the cutoff parameter in all physical processes. The technique to accommodate infrared confinement is fairly versatile and can be applied to quark diagrams having any number of loops and propagators. In addition, the confinement scenario enables us to incorporate all conceivable resonance states in our computations. As a result, infrared cut-off parameter guarantees confinement. Here it should be emphasized that the above method is widely generalized and can be used for diagrams having n number of loops and propagators.

Although the CCQM is not based on first principle methods, the calculations shown by authors of [115] demonstrate that a wide variety of low energy mesonic processes can be consistently described by using only few tunable parameters namely, size parameter Λ_H, constituent quark masses m_i and infrared confinement constant λ. Uncertainty in the quark masses are not included because they are the part of the model parameters so we want to keep them as they were fixed/tuned while designing the model. That will help us to maintain the universality of the model for different systems. Model parameters are listed in the Tab. 2.2. All tunable parameters mentioned above are obtained by fitting the radiative decay constants to experimental data or taken from LQCD calculations 3.18. With obvious modifications, CCQM can also be used to study baryonic decay processes.

In the next chapter, we use CCQM to calculate weak semileptonic decays of open flavor mesons.

Table 2.1: Leptonic decay constant f_H (in MeV)

f_H	Present	Data	Refrences
f_D	206.08	202.2(2.2)(2.6)	LQCD [?]
		210 ± 11	QCDSR [?]
		211.9(1.1)	PDG [12]
f_{Ds}	257.70	258.7 (1.1) (2.9)	LQCD [?]
		259 ± 10	QCDSR [?]
		249.0(1.2)	PDG [12]
f_{Ds}/f_D	1.25	1.173(3)	PDG [12]
f_K	156.96	155.37(34)	LQCD [?]
		157.9 ± 1.5	LQCD [?]
		155.6(0.4)	PDG [12]
f_π	130.30	130.39 (20)	LQCD [?]
		132.3 ± 1.6	LQCD [?]
		130.2(1.7)	PDG [12]
f_K/f_π	1.20	1.1928(26)	PDG [12]
f_{D^*}	244.27	$278. \pm 13 \pm 10$	LQCD [?]
		263 ± 21	QCDSR [?]
$f_{D_s^*}$	272.08	311 ± 9	LQCD [?]
		308 ± 21	QCDSR [?]
f_{K^*}	226.81	222 ± 8	QCDSR [?]
f_ρ	218.28	$208.5 \pm 55 \pm 0.9$	LQCD [?]
f_ϕ	226.56	238 ± 3	LQCD [?]
		215 ± 5	QCDSR [?]
f_ω	198.38	194.6 ± 3.24	LFQM [8]

Table 2.2: CCQM model parameters: quark masses, meson size parameters and infrared cut-off parameter (all in GeV)

Λ_B	Λ_{B_s}	Λ_π	$\Lambda_{\bar{K}^0}$	Λ_ρ	$\Lambda_{\bar{K}^{*}(892)^0}$	Λ_{Ds}
1.963 ± 0.038	2.05 ± 0.036	0.871 ± 0.002	1.014 ± 0.008	0.610 ± 0.012	0.81 ± 0.024	1.75 ± 0.035
$m_{u/d}$	m_s	m_c	m_b	λ	Λ_ω	Λ^*_{Ds}
0.241	0.428	1.67	5.05	0.181	0.488 ± 0.019	1.56 ± 0.014